

Mechanistic insight into catalytic conversion of methane on $\text{Sr}_2\text{Fe}_{1.5}\text{Mo}_{0.5}\text{O}_6$ perovskite anode: A combined EIS-DRT, DFT and TPSR investigation

Zongying Han^{a,*}, *Hui Dong*^b, *Yuhao Wang*^c, *Yanru Yang*^a, *Hao Yu*^a, *Zhibin Yang*^{d,**}

^a College of Energy Storage Technology, Shandong University of Science and Technology, Qingdao 266590, China

^b College of Chemical and Biological Engineering, Shandong University of Science and Technology, Qingdao 266590, China

^c Department of Mechanical and Aerospace Engineering, The Hong Kong University of Science and Technology, Clear Water Bay, Hong Kong SAR, China

^d Research Center of Solid Oxide Fuel Cell, China University of Mining & Technology-Beijing, Beijing, 100083, China

* Corresponding author. Email address: hzy5315@163.com (Z.Y. Han)

** Corresponding author. Email address: yangzhibin0001@163.com (Z.B. Yang)

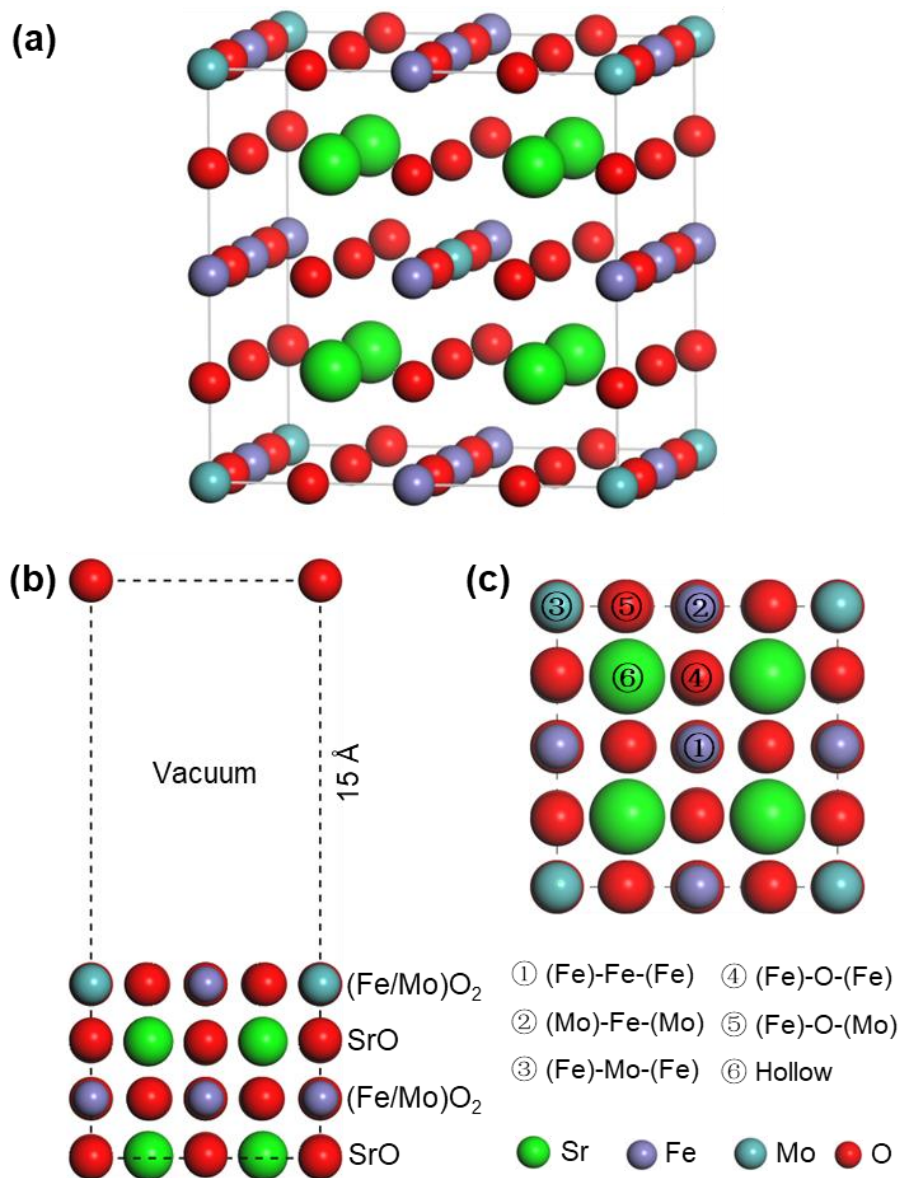


Fig. S1 SFMO bulk model (s), SFMO (001) surface model (b) and potential adsorption sites (c) on SFMO (001) surface.

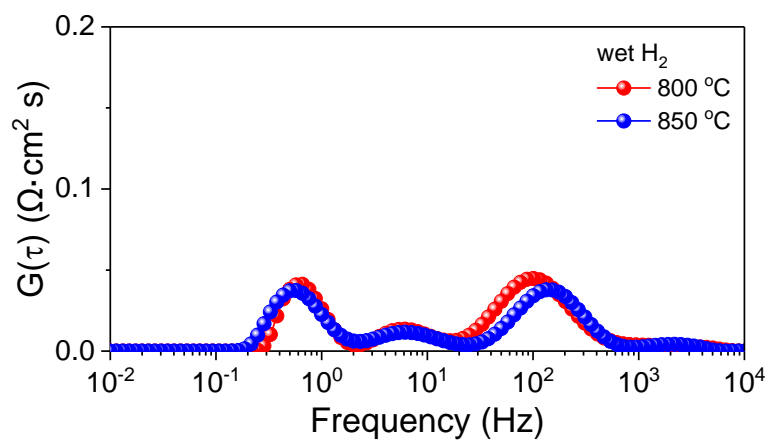


Fig. S2 DRT curves of the SFM/LSGM/LSCF cell in wet hydrogen fuel.

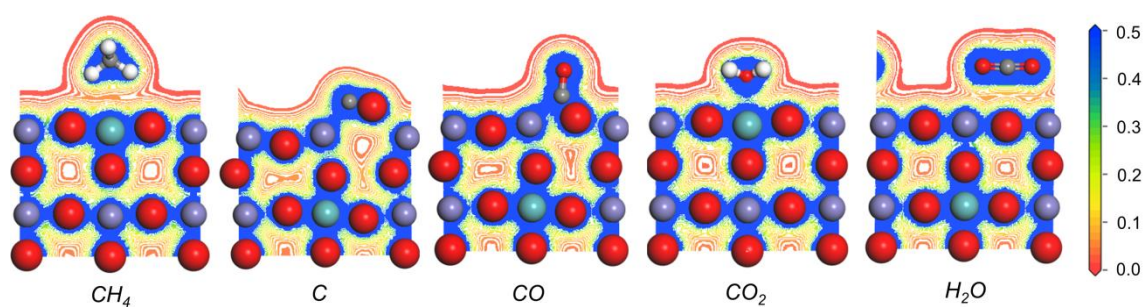


Fig. S3 Electron density distribution in the most stable adsorption configurations of the key species on SFMO (001) surface. Electron density is given in units of electrons per \AA^3 .

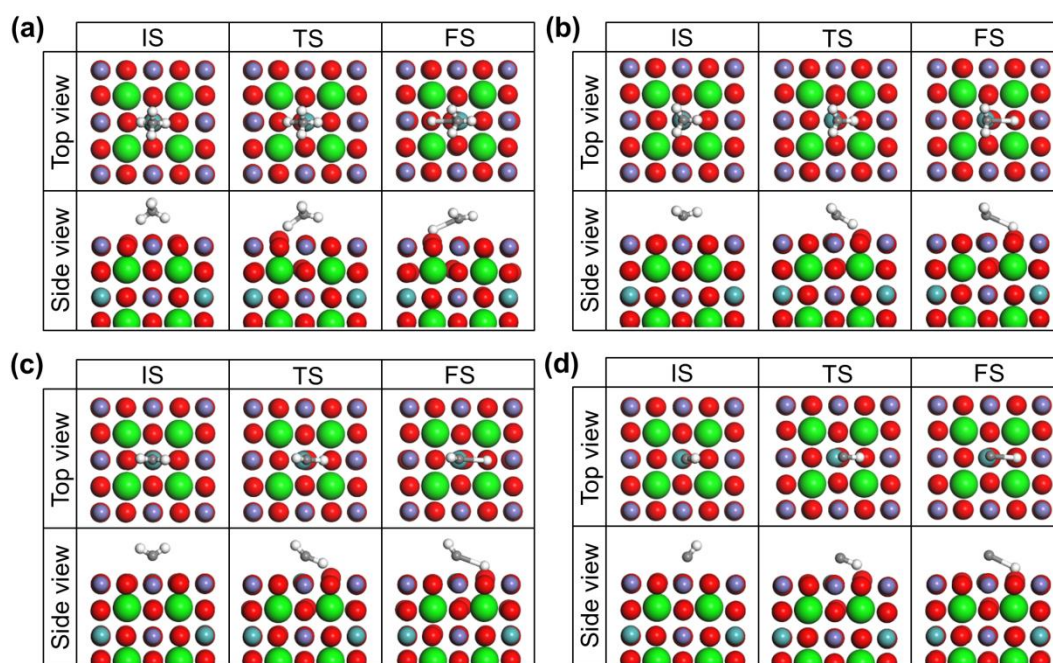


Fig. S4 Geometry of the IS, TS and FS of methane cracking on the (Fe)-Mo-(Fe) site over SFMO surface. (a) $\text{CH}_4 = \text{CH}_3 + \text{H}$; (b) $\text{CH}_3 = \text{CH}_2 + \text{H}$; (c) $\text{CH}_2 = \text{CH} + \text{H}$; (d) $\text{CH} = \text{C} + \text{H}$.

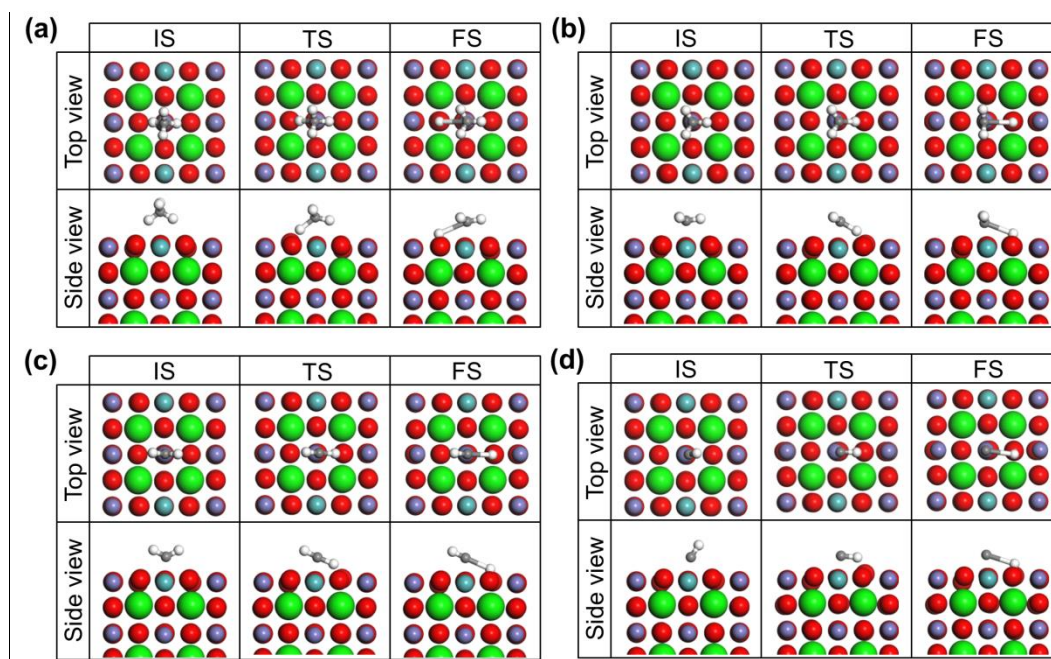


Fig. S5 Geometry of the IS, TS and FS of methane cracking on the (Mo)-Fe-(Mo) site over SFMO surface. (a) $\text{CH}_4 = \text{CH}_3 + \text{H}$; (b) $\text{CH}_3 = \text{CH}_2 + \text{H}$; (c) $\text{CH}_2 = \text{CH} + \text{H}$; (d) $\text{CH} = \text{C} + \text{H}$.

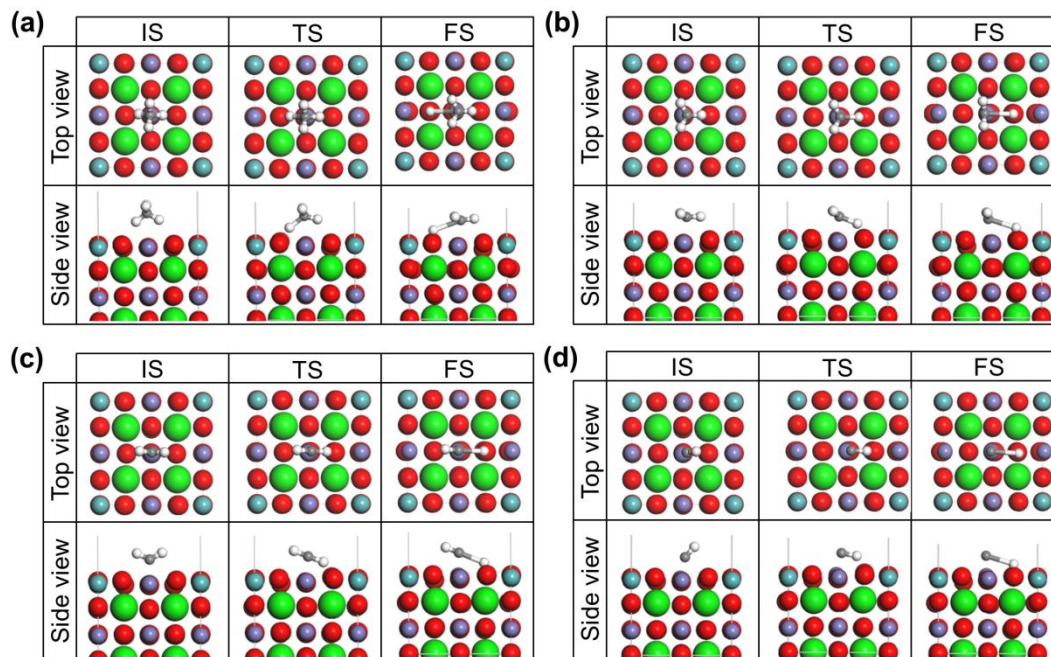


Fig. S6 Geometry of the IS, TS and FS of methane cracking on the (Fe)-Fe-(Fe) site over SFMO surface. (a) $\text{CH}_4 = \text{CH}_3 + \text{H}$; (b) $\text{CH}_3 = \text{CH}_2 + \text{H}$; (c) $\text{CH}_2 = \text{CH} + \text{H}$; (d) $\text{CH} = \text{C} + \text{H}$.

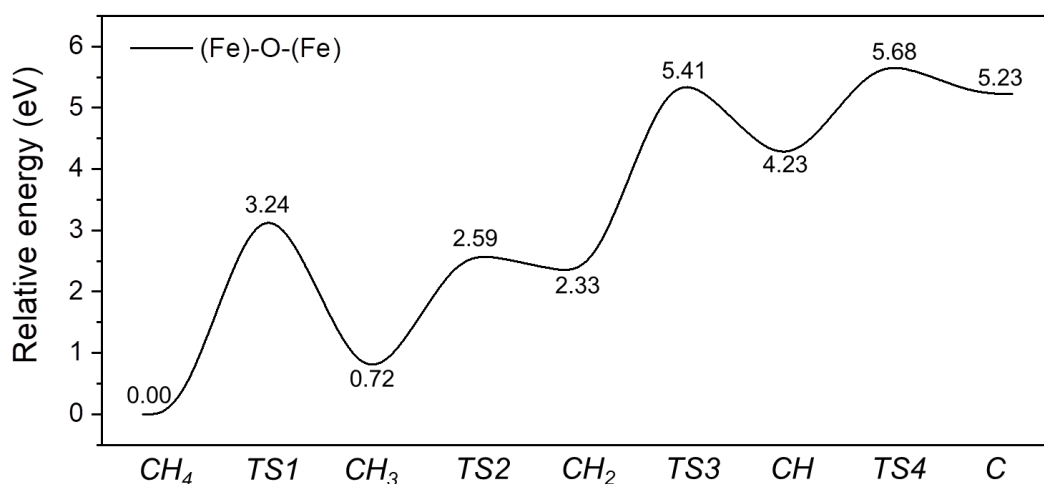


Fig. S7 Energy profile of methane cracking on surface oxygen site of SFMO (001) surface.

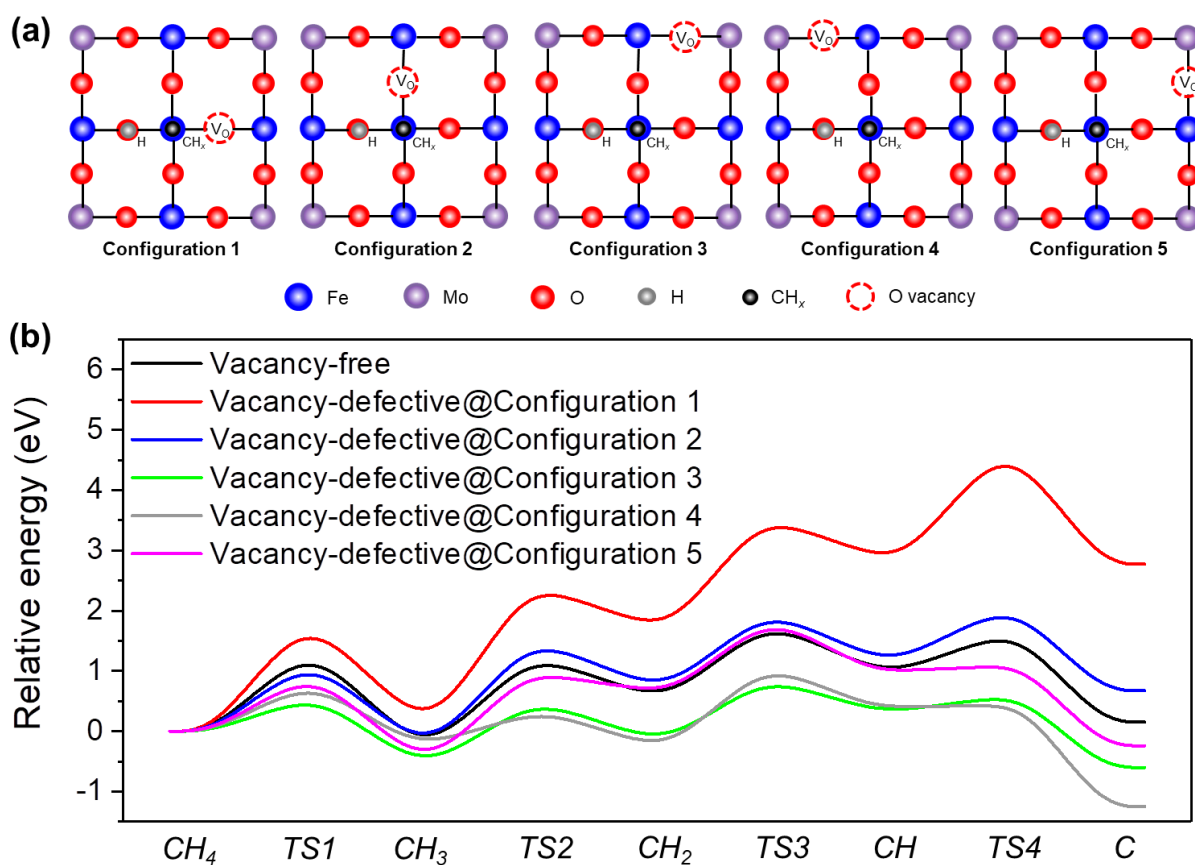


Fig. S8 (a) Schematic diagram of five type of methane cracking configurations on the preferred surface (Fe)-Fe-(Fe) site of oxygen vacancy-defective SFMO surface; (b) Comparison of the energy profiles of methane cracking on the preferred surface (Fe)-Fe-(Fe) site with and without oxygen vacancy.

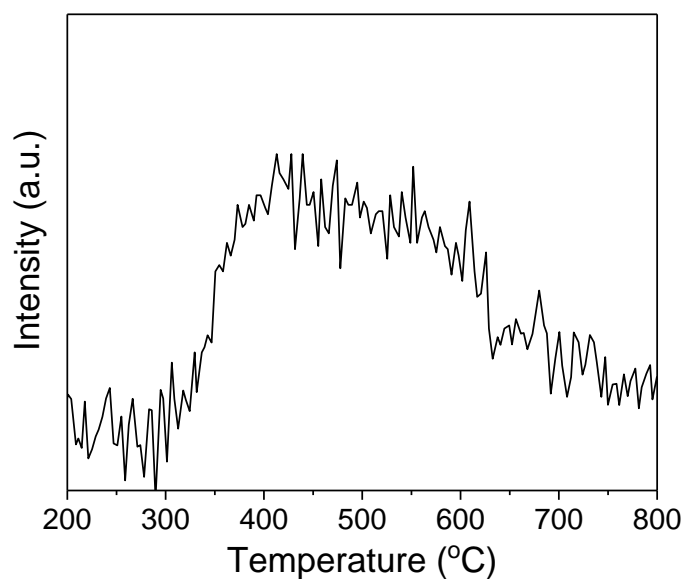


Fig. S9 The CH₄ desorption profile over the as-synthesized SFMO perovskite.

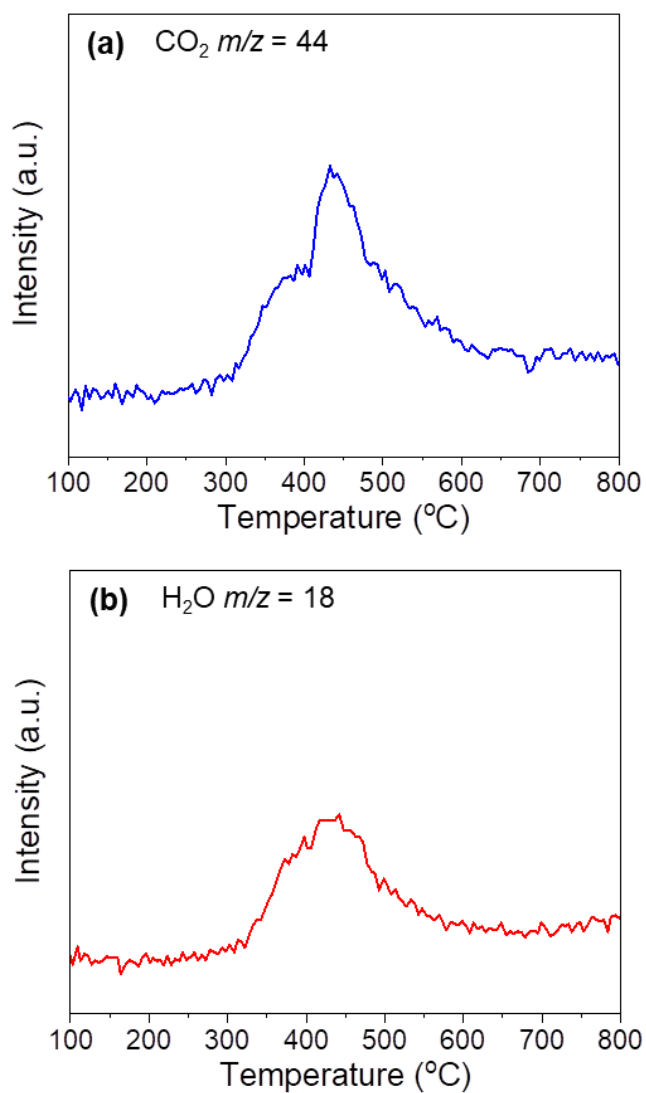


Fig. S10 CH₄-TPSR profiles corresponding to the reaction of CH₄ and lattice oxygen over Ni-YSZ as function of temperature.

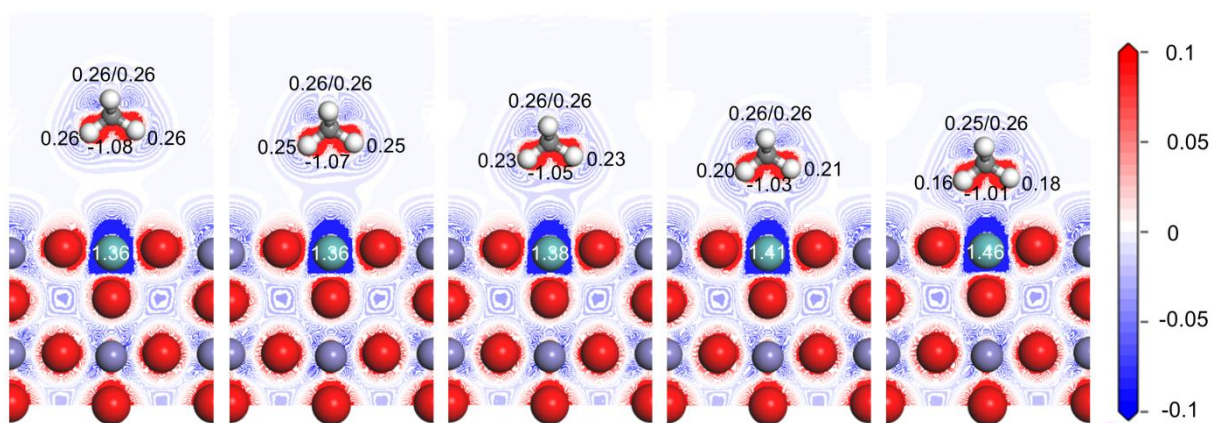


Fig. S11 Electron density differences as the methane molecule approaches the surface given in units of electrons per \AA^3 . In this plot a loss of electrons is indicated in blue, while electron enrichment is indicated in red. Inserted values represent the Mulliken charge of H and C atoms in CH_4 molecule and the beneath Mo atom on the surface.